Detecting handedness of spatially oriented molecules by Coulomb explosion imaging

Cem Saribal,[1,2] Alec Owens,[3] Andrey Yachmenev,[1,4,a)] and Jochen Küpper[1,2,4]
[1)] *Center for Free-Electron Laser Science, Deutsches Elektronen-Synchrotron DESY, Notkestraße 85, 22607 Hamburg, Germany*
[2)] *Department of Physics, Universität Hamburg, Luruper Chaussee 149, 22761 Hamburg, Germany*
[3)] *Department of Physics and Astronomy, University College London, Gower Street, London WC1E 6BT, United Kingdom*
[4)] *The Hamburg Center for Ultrafast Imaging, Universität Hamburg, Luruper Chaussee 149, 22761 Hamburg, Germany*

(Dated: 2021-01-11)

We present a new technique for detecting chirality in the gas phase: Chiral molecules are spatially aligned in three-dimensions by a moderately strong elliptically-polarized laser field. The momentum distributions of the charged fragments, produced by laser-induced Coulomb explosion, show distinct three-dimensional orientation of the enantiomers, when the laser polarization ellipse is rotated by a non-right angle with respect to the norm vector of the detector plane. The resulting velocity-map-image asymmetry is directly connected to the enantiomeric excess and to the absolute handedness of molecules. We demonstrated our scheme computationally for camphor ($C_{10}H_{16}O$), with its methyl-groups as marker fragments, using quantum-mechanical simulations geared toward experimentally feasible conditions. Computed sensitivity to enantiomeric excess is comparable to other modern chiroptical approaches. The present method can be readily optimized for any chiral molecule with an anisotropic polarizability tensor by adjusting the polarization state and intensity profile of the laser field.

Chiral molecules exist in structural forms known as enantiomers, which are mirror images of one another that are non-superimposable by translation and rotation. The chemical behavior of molecular enantiomers can be profoundly different. Particularly in the pharmaceuticals industry, methods to differentiate between them or to determine the enantiomeric excess (*ee*) of a chiral sample are important. In recent years, there have been considerable advances in gas-phase chiroptical techniques and a variety of such methods have emerged, for example, using phase-sensitive microwave spectroscopy,[1,2] Coulomb explosion imaging with coincidence detection,[3,4] photoelectron circular dichroism (PECD),[5–9] chiral-sensitive high-harmonic generation,[10–12] or attosecond-time-resolved photoionization.[13] These approaches offer improved sensitivity and their success is based on exploiting electric-dipole interactions for chiral discrimination,[14] producing stronger signals than circular dichroism from magnetic-dipole interactions.

Coulomb explosion imaging is a powerful and efficient approach to retrieve the instantaneous absolute structures of complex molecules.[15–17] Applied to chiral molecules, coincident imaging of fragments emitted from the chiral center can be used to determine the handedness of their enantiomers, in the conceptually most straightforward way by coincident detection of all fragments attached to the stereocenter.[3,4] For axially chiral molecules, it has been demonstrated that it is sufficient to only correlate two different fragments, if the molecules are pre-aligned along their axis of chirality.[18]

For molecular enantiomers placed in a field coupling two molecular dipole moment projections or two off-diagonal polarizability elements it was demonstrated that they exhibit transient dipole moments and spatial orientations with opposite sign for the different enantiomers.[1,19–22] Experiments inducing enantiomer-specific orientation, e. g., probed by Coulomb explosion imaging, were reported, albeit so far with very low sensitivity to the enantiomeric excess.[22]

Here, we explore the effect of spatial three-dimensional (3D) alignment of molecules in Coulomb explosion imaging in order to sensitively probe the *ee* and the handedness of chiral molecules with it. Using accurate computational procedures, we demonstrate that 3D alignment by an elliptically-polarized non-resonant field can break the symmetry in a fragments position and momentum distribution in the detector plane, if the polarization ellipse is tilted by an angle $0 < \beta < 90\,^\circ$ with respect to the norm vector of the detector. The asymmetry between the detector's left and right halfs gives access to the *ee* and handedness of chiral molecules. This method is more robust than previous Coulomb-explosion-based approaches, e. g., regarding detector limitations and experimental imperfections. Our theoretical estimates for the sensitivity to the *ee* are comparable to other modern chiroptical techniques, such as PECD. To further enhance sensitivity we also explore the effect of one-dimensional (1D) orientation combined with 3D alignment.

Figure 1 illustrates the underlying idea of our approach, which is demonstrated for the prototypical chiral molecule camphor ($C_{10}H_{16}O$). A non-resonant elliptically-polarized laser field is applied to achieve 3D alignment. The most polarizable axis of the molecule p is aligned along the major axis Z_L of the elliptical field and the second most

[a)] Email: andrey.yachmenev@cfel.de; URL: https://www.controlled-molecule-imaging.org

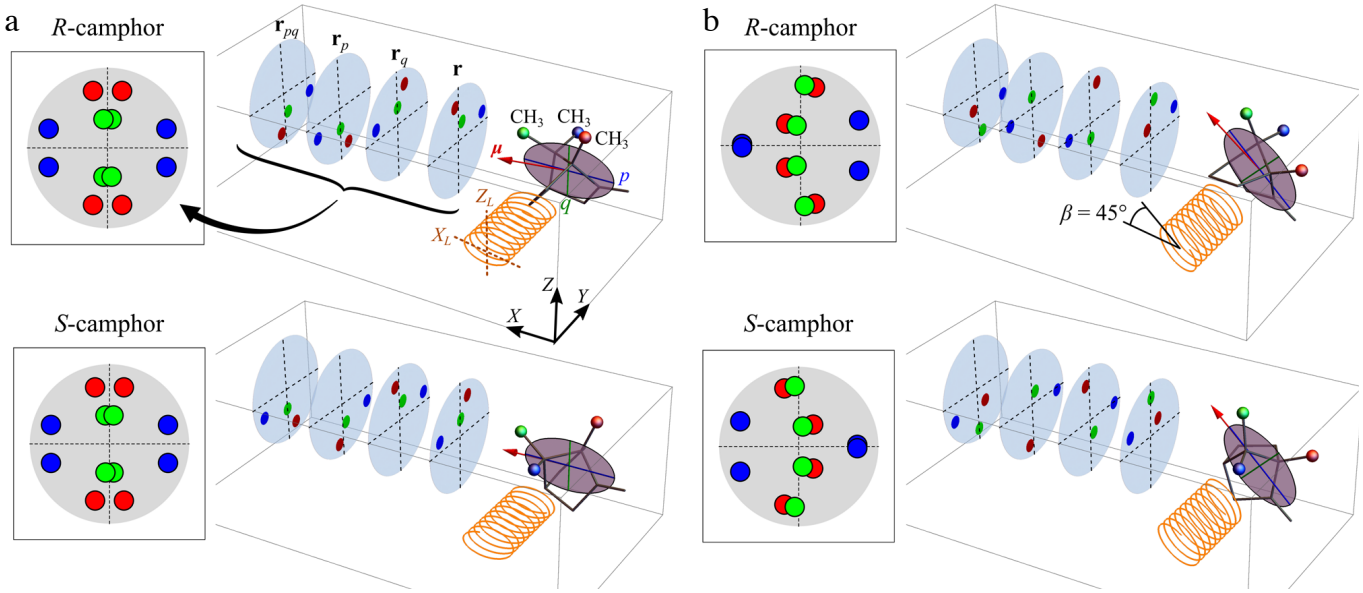

FIG. 1. Sketch of the 3D alignment of the R and S enantiomers of camphor by an elliptically-polarized laser field and corresponding projections of its methyl groups onto the detector. The most polarizable axes p and q ($\alpha_p > \alpha_q$) of the molecule are aligned along the major Z_L and minor X_L axes of the elliptical field, and the four different projections of the methyl groups onto the plane of the detector correspond to the four equivalent molecular orientations in the $(X_\mathrm{L}, Z_\mathrm{L})$ plane. (a) When either of the X_L or Z_L axes is perpendicular to the plane of the detector, the sum of the different methyl-group projections look exactly the same for the different enantiomers. (b) However, the projections differ when the polarization ellipse is rotated by a non-right angle $\beta \neq n \cdot 90\,^\circ$, $n = 0, 1, 2, \ldots$; see (1) for the definition of the $\mathbf{r}$ vectors.

polarizable axis q along the minor elliptical axis X_L. We chose the three distinct methyl (CH_3) groups in camphor as marker fragments to differentiate between the R and S enantiomers in a Coulomb-explosion imaging. Their flight directions can be observed experimentally as momentum distributions of the CH_3^+ ions resulting from multiple ionization followed by Coulomb explosion of the molecule.[23,24]

We assume that two-body dissociation events produce equal initial momenta for CH_3^+ fragments at three different molecular sites. By normalizing the size of the Newton sphere to one, the momenta distributions are given by the position distributions of the CH_3 groups. These methyl-group distributions in the detector plane are schematically plotted in Figure 1 for the idealized case of perfect 3D alignment. Fixed in the $X_\mathrm{L}Z_\mathrm{L}$ laser polarization plane, the molecule orients itself in one of four equally preferred ways, which are related by 180 ° rotations about the most polarizable p and q axes of the molecule. Fixing the plane of elliptical polarization in the XZ laboratory plane, the cartesian coordinates of an atom in the molecule projected onto the YZ plane of the detector for all four possible spatial molecular orientations are given by

$$\begin{aligned}
\mathbf{r} &= \big(+y, +(z\cos\beta - x\sin\beta)\big)\\
\mathbf{r}_p &= \big(-y, +(z\cos\beta + x\sin\beta)\big)\\
\mathbf{r}_q &= \big(-y, -(z\cos\beta + x\sin\beta)\big)\\
\mathbf{r}_{pq} &= \big(+y, -(z\cos\beta - x\sin\beta)\big)
\end{aligned} \qquad (1)$$

where x, y, z denote the cartesian coordinates of an atom in the principal-axis-of-polarizability frame of the molecule. The subscript indices p and q denote cartesian vectors obtained by 180 ° rotations about the respective molecular polarizability axes, which in the case of perfect 3D alignment coincide with the Z_L and X_L axes of the polarization ellipse. The angle β is the angle between the major Z_L axis of the ellipse and the norm ($\mathbf{e}_X$) of the detector. It describes the rotation of the polarization ellipse about the Y axis.

The four different positions $\mathbf{r}$, $\mathbf{r}_p$, $\mathbf{r}_q$ and $\mathbf{r}_{pq}$ in the plane of the detector are plotted in Figure 1 for the three carbon atoms that belong to the methyl-groups for R and S camphor. Different enantiomers have opposite signs of the Y component of each position vector in (1). When $\beta = n \cdot 90\,^\circ$, $n = 0, 1, 2, \ldots$ the four different positions in the plane of the detector for each atom produce an image, which is symmetric with respect to the inversion of both Y and Z axes, as shown in Figure 1 a. Since the position vectors for the R and S enantiomers differ only in the sign of the Y coordinate, the resulting projections will look exactly the same for different enantiomers. However, when $\beta \neq n \cdot 90\,^\circ$ the symmetry with respect to the inversion of the Y axis in (1) will be broken. As a result, the sums of the four equivalent molecular spatial orientations will exhibit distinctly different projections on the detector plane for the R and S enantiomers, see Figure 1 b. The detector images of the enantiomers are asymmetric with respect to the left and right parts and are in fact mirror

images of each other for the enantiomers. This allows for the determination of the *ee* and the handedness of chiral molecules. Notably, the present approach does not require coincidence measurements of different fragment species.

To benchmark our scheme we performed quantum-mechanical calculations of the rotational dynamics of camphor using the accurate variational procedure Rich-Mol,[25] which simulates the rotation-vibration dynamics of molecules in the presence of external fields. The field-free rotational motion was modelled using the rigid-rotor Hamiltonian with the rotational constants $A = 1446.968977$ MHz, $B = 1183.367110$ MHz, and $C = 1097.101031$ MHz.[26] Simulations of the field-induced time-dependent quantum dynamics employed wave packets built from superpositions of field-free eigenstates including all rotational states of the molecule with $J \leq 40$, where J is the quantum number of overall angular momentum. Only the vibrational ground-state was considered, reflecting the conditions in a cold molecular beam. The time-dependent coefficients were obtained by numerical solution of the time-dependent Schrödinger equation using the time-discretization method with a time step of $\Delta t = 10$ fs and a Lanczos-based approach for the time-evolution operator.[27]

The field interaction potential was represented as a multipole moment expansion of order up to the polarizability interaction tensor. The dipole moment and polarizability tensor were calculated using the coupled cluster method CCSD(T) with the augmented correlation-consistent basis set aug-cc-pVTZ[28,29] in the frozen-core approximation. The calculations were performed at the experimentally determined molecular geometry[26] using CFOUR.[30]

The long elliptically-polarized laser pulse was represented as

$$E(t) = E_0\sqrt{4\log 2/(\pi\tau^2)}\ \exp\left(-4\log 2(t-t_0)^2/\tau^2\right) \times \left[(\cos(\omega t)\cos\beta + \frac{1}{\sqrt{3}}\sin(\omega t)\sin\beta)\mathbf{e}_X + (\cos(\omega t)\sin\beta - \frac{1}{\sqrt{3}}\sin(\omega t)\cos\beta)\mathbf{e}_Z\right] \quad (2)$$

with the parameters $E_0 = 4\times10^9$ V/cm, corresponding to a laser peak intensity $I = 6\times10^{11}$ W/cm^2, $\omega = 800$ nm, $t_0 = 440$ ps, and $\tau = 250$ ps. The calculations were performed for β angles ranging from 0 to 90°. For some calculations we added the interaction between the permanent molecular dipole moment and a static electric field of 1 or 5 kV/cm aligned along the detector norm vector $\mathbf{e}_X$. A hypothetical strong probe pulse, causing the Coulomb explosion, was applied at a time $t = 440$ ps corresponding to the peak intensity of the alignment field. Idealized simulations were performed at an initial rotational temperature of $T = 0$ K, and for experimentally realistic conditions at $T = 0.2$ K. Sub-Kelvin rotational temperatures can routinely be achieved using carefully optimized supersonic expansions,[31–33] molecular beams coupled to the electrostatic deflector[34–36] or focusers.[37–39] Alternatively, helium nanodroplets provide comparably low temperatures of 0.4 K[40] and allow for similar Coulomb explosion imaging experiments of aligned molecules,[41] including some large and complex systems.[42] Beyond that, buffer-gas cooled molecular beams provide molecules in the gas phase at temperatures down to ∼1 K[43] or using dilution refrigerators even at <0.5 K.[44] Such buffer-gas-cooled beams were demonstrated for complex molecules[45] and recently extended to arbitrarily large molecular systems and nanoparticles.[46]

The degree of 3D alignment is characterized by $\langle\cos^2\theta_{p,Z_L}\rangle = 0.84$ and $\langle\cos^2\theta_{q,X_L}\rangle = 0.76$ for $T = 0$ K. For a finite initial temperature of $T = 0.2$ K we obtained $\langle\cos^2\theta_{p,Z_L}\rangle = 0.64$ and $\langle\cos^2\theta_{q,X_L}\rangle = 0.50$.

The distributions of the methyl-group fragments of camphor in the YZ detector plane were simulated by computing the probability density distributions of the corresponding carbon atoms using the rotational wavepackets at the peak of the laser pulse. The total distribution was modelled as a normalized sum of contributions from the three individual methyl-group carbon atoms with equal weights. As the recoil axes, we chose vectors along the molecular bonds connecting the carbon atoms in the methyl groups with the backbone of the molecule. To account for non-axial recoil, the calculated probability density distributions of the methyl-group carbon atoms were convoluted with a Gaussian function of a solid angle representing angular displacement from the recoil vector. The full-width at half maximum (FWHM) parameter of the Gaussian function was chosen at 30 °, which is near typical experimental values.[47]

Figure 2 a shows the calculated 2D projections of the probability density distributions for the carbon atoms in the methyl groups of R and S camphor for different β angles and an initial rotational temperature of $T = 0$ K. As expected, for $\beta = 0, 90$ °, the 2D projections are symmetric with respect to inversion of Y and Z axes. Thus, their averages for the four orientation look identical for the different enantiomers. The 2D density projections become asymmetric with respect to inversion of the Y axis for intermediate values of the β angle. In Figure 2 a the results are shown for $\beta = 30°$ and 60°. For different enantiomers the distributions are exact mirror images of each other in the YZ plane. For racemic mixtures, the 2D density, and consequently the momentum projections of the methyl-group fragments, will be symmetric to inversion of the Y axis, and the presence of an asymmetry between the left and right halfs of the detector will thus indicate the *ee*.

To identify the parts of the detector images, which have the largest asymmetry and are therefore most sensitive to the *ee*, we propose to define an asymmetry parameter as a normalized difference $\mathcal{A}(\theta) = [N_\Omega(\theta) - N_\Omega(-\theta)]/[N_\Omega(\theta) + N_\Omega(-\theta)]$ between sectors in the right and left halfs of the detector. Here, $N_\Omega(\theta)$ is the intensity in an angular sector of fixed width Ω at $\theta = 0\ldots180$ °, i. e., in the right half of the detector. Thus, $N_\Omega(-\theta)$ is the corresponding

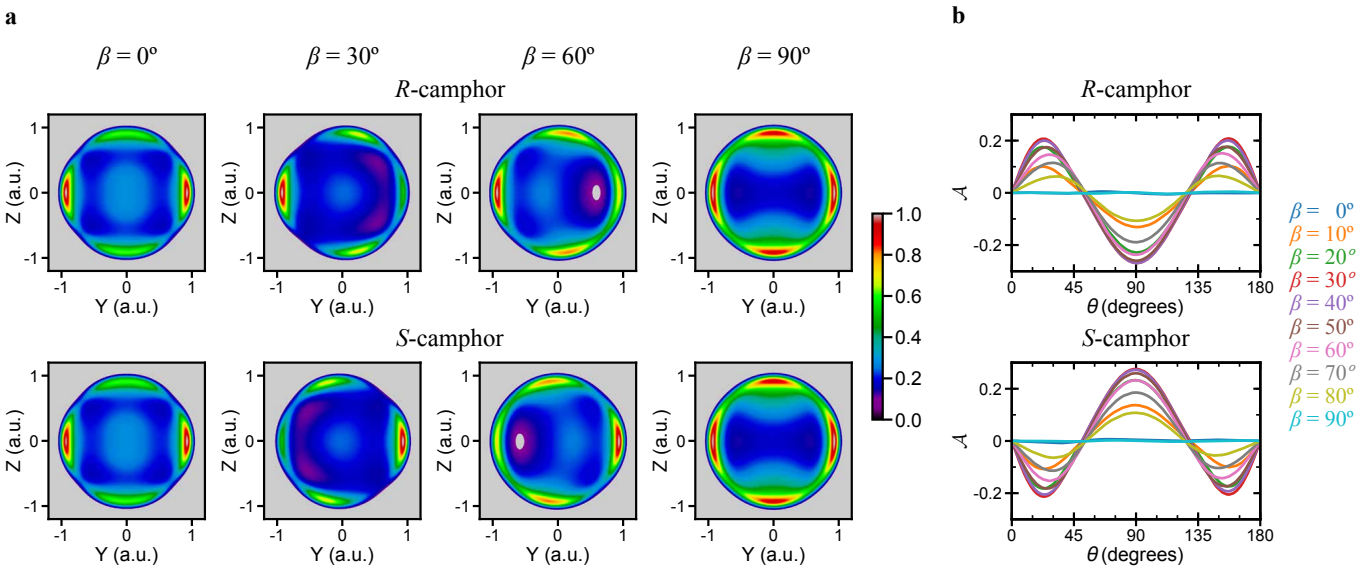

FIG. 2. (a) Computed 2D projections of the averaged probability density distributions of the carbon atoms in the methyl groups of R and S camphor at the peak of the alignment field and an initial rotational temperature of $T = 0$ K. (b) Asymmetry parameter $\mathcal{A}$ as a function of the θ angle. The results are shown for angles $\beta = 0, 30, 60, 90\,^\circ$ between the major axis a of the elliptical field and the norm vector of the detector plane.

intensity in the left half of the detector. The asymmetry $\mathcal{A}(\theta)$ is linearly dependent on the *ee*: it is zero for the racemic mixture and attains its maximum value for the pure enantiomer. The asymmetry $\mathcal{A}(\theta)$ for $\Omega = 30\,^\circ$ for different β is shown in Figure 2 b. The largest value of $\mathcal{A}$ for the R and S enantiomers, respectively, are obtained as $\mathcal{A} \approx 0.22$ for $\beta = 30 \ldots 50\,^\circ$ and $\mathcal{A} \approx -0.3$ for $\theta = 90°$.

Generally, the asymmetry values $\mathcal{A}$ depend on the molecule, its marker fragments, and their recoil axes with respect to the alignment plane. In the case of a large number of indistinguishable fragment groups attached at various molecular sites, e.g. hydrogen atoms,[48] the total probability density will look more isotropic, even for strong 3D alignment. The degree of angular asymmetry will also be lowered when looking at fragments dissociating in directions nearly co-planar to either the alignment plane or the plane of detector.

In the present case, there are three indistinguishable CH_3 fragments attached at different sites of camphor. The optimal value of the β angle can be thought of as the one that maximizes the overlap of the 2D probability density distributions of different CH_3 fragments. This leads to a more anisotropic total density distribution and a better contrast with respect to variaton of θ.

The magnitude of angular asymmetry $\mathcal{A}(\theta)$ also depends on the degree of 3D alignment. The lower degree of alignment for a 0.2 K sample leads to more diffuse 2D projections of the probability density distributions and, therefore, to smaller values of asymmetry $\mathcal{A}(\theta)$. These are plotted in Figure 3 for a selected optimal value of $\beta = 40°$. The maximum value of $\mathcal{A}(\theta = 90\,^\circ) = \pm 0.1$ at $T = 0.2$ K is decreased by a factor of three as compared to the $T = 0$ K results. For higher temperatures close to 1 K, the asymmetry drops further by a factor of 5.3. The loss of asymmetry will vary for different molecules depending on the density of rotational states as well as their polarizability anisotropy. The present estimates of the maximum asymmetry for cold ($T \leq 0.4$ K) molecular beams of camphor are comparable to those achieved in PECD experiments, where the asymmetry is defined as the normalized difference between the number of electrons emitted by the molecule in the forward and backward hemispheres relative to the laser beam.[7] Fenchone, for example, a chiral molecule with a structure similar to the one of camphor, showed an asymmetry value of ± 0.15 in PECD experiments.[8] A key advantage of our approach over methods such as PECD or microwave three-wave mixing is access to the absolute handedness of the *ee*. Indeed, the position of the methyl groups with respect to the plane of 3D alignment is unique for the R and S enantiomers. As a result, the absolute sign of the left-right asymmetry in the ion momentum distributions can be unambiguously assigned to the enantiomer's absolute configuration. Notably, in order to predict the absolute sign of the asymmetry parameter in the axial recoil approximation it is sufficient to know the geometry of the molecule and its polarizability tensor, where only relative magnitudes of tensor elements matter.

One may consider to increase the degree of asymmetry by rendering the four equivalent alignment orientations of unequal probability. This can be achieved, for instance, by applying a dc electric field along the norm vector of the detector plane, known as mixed-field orientation.[38,49–51] We calculated the asymmetry $\mathcal{A}(\theta)$ for dc field strengths of 1 and 5 kV/cm at $T = 0$ K, shown in Figure 4; note that $\mathcal{A}(S) = -\mathcal{A}(R)$. As the dc field breaks the symmetry

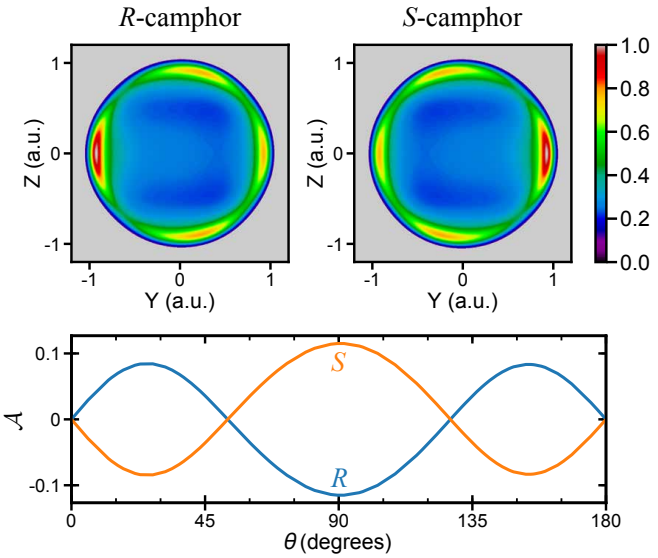

FIG. 3. Computed 2D projections of the averaged probability density distributions for carbon atoms in the methyl groups of R and S camphor at the peak of the alignment field and an initial rotational temperature of $T = 0.2$ K. On the bottom panel, the asymmetry parameter $\mathcal{A}$ as a function of the θ angle for both enantiomers is displayed. The results are shown for the optimal value of $\beta = 40°$.

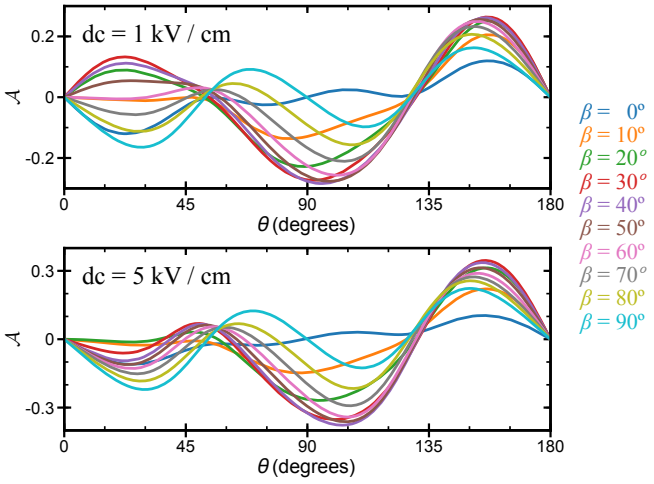

FIG. 4. Effect of the dc field on the asymmetry of the 2D projections of the averaged probability density distributions for carbon atoms in the methyl groups of R-camphor, computed at the peak of the alignment field for different values of β and an initial rotational temperature of $T = 0$ K.

with respect to the inversion of Y and Z axes, although the simultaneous inversion of both axes is still symmetric, the non-zero asymmetry can be observed even at $\beta = 0, 90\,°$. The maximal degree of asymmetry increases up to ± 0.4 with increasing dc field strength, the effect however quickly saturates at stronger dc fields.[34,50] The absolute sign of the asymmetry, defined as the difference between the left and right halfs of the detector, as well as the optimal values of β and θ remain the same as for pure alignment. This is rationalized by the fact that the mixed-field orientation in camphor still allows for two of the four orientations producing the effect of 3D alignment with 1D orientation.[52] The mixed-field orientation effect however can only be achieved for polar molecules with a non-vanishing projection of the dipole moment onto the pq plane of the most polarizable axes.

In conclusion, we demonstrated a novel and robust approach for detecting chirality based on the Coulomb explosion imaging of 3D aligned molecules. The method employs elliptically polarized non-resonant laser pulses in a standard setup as is typically used for studying molecular alignment.[53,54] The chirality is revealed by an asymmetry in the 2D projections of ion momentum distributions. This paves the way to the sensitive analytic use of Coulomb explosion imaging for detecting the *ee* with a sensitivity comparable to PECD.[7,8,55] Any molecule with three different principal polarizability components can be investigated this way. We note that, different from PECD, our technique requires strong alignment that is typically achieved by utilizing cold molecular beams.

Although we found that for camphor the methyl-group fragments deliver sufficient asymmetry, these fragments could possibly exhibit larger non-axial recoil velocities not fit by the Gaussian-distribution model assumed. This would result in additional smearing effects on the structures in the ion momentum distributions. Thus, the present approach is best suited for chiral molecules with nearly-axially-recoiling leaving groups, but could be extended further through a more general analysis based on time-resolved measurements.[48]

When compared to existing coincidence Coulomb explosion imaging techniques, our approach can distinguish between the left- and right-handed enantiomers without correlated detection of multiple different fragments.[3,4,18] This enables much faster data acquisition, which is highly advantageous for ultrafast time-resolved studies. For the present method, the asymmetry signal quickly declines with the beam temperature, with the efficiency similar to coincident imaging at $\sim$1 K. The advantage however is that, in principle, only one fragment type is necessary to detect chirality and handedness, as opposed to standard methods demanding up to five different fragments. The external fields can be further optimized to improve the sensitivity. In particular, we demonstrated that mixed-field orientation can be exploited to enhance the asymmetry in the ion momentum distributions and thus the method's *ee* sensitivity. The approach could be combined with PECD in ion-electron coincidence measurements[56] to extract the *ee* from the photo-electron distributions together with the handedness obtained from the ion momentum distributions.

This work has been supported by the Deutsche Forschungsgemeinschaft (DFG) through the priority program "Quantum Dynamics in Tailored Intense Fields" (QUTIF, SPP1840, KU 1527/3, YA 610/1) and the cluster of excellence "Advanced Imaging of Matter" (AIM,

EXC 2056, ID 390715994).

The data that support the findings of this study are available from the corresponding author upon request.

[1] D. Patterson, M. Schnell, and J. M. Doyle, "Enantiomer-specific detection of chiral molecules via microwave spectroscopy," Nature **497**, 475–477 (2013).

[2] S. R. Domingos, C. Pérez, and M. Schnell, "Sensing chirality with rotational spectroscopy," Annu. Rev. Phys. Chem. **69**, 499–519 (2018).

[3] M. Pitzer, M. Kunitski, A. S. Johnson, T. Jahnke, H. Sann, F. Sturm, L. P. H. Schmidt, H. Schmidt-Böcking, R. Dörner, J. Stohner, J. Kiedrowski, M. Reggelin, S. Marquardt, A. Schießer, R. Berger, and M. S. Schöffler, "Direct determination of absolute molecular stereochemistry in gas phase by Coulomb explosion imaging," Science **341**, 1096–1100 (2013).

[4] P. Herwig, K. Zawatzky, M. Grieser, O. Heber, B. Jordon-Thaden, C. Krantz, O. Novotný, R. Repnow, V. Schurig, D. Schwalm, Z. Vager, A. Wolf, O. Trapp, and H. Kreckel, "Imaging the absolute configuration of a chiral epoxide in the gas phase," Science **342**, 1084–1086 (2013).

[5] N. Böwering, T. Lischke, B. Schmidtke, N. Müller, T. Khalil, and U. Heinzmann, "Asymmetry in photoelectron emission from chiral molecules induced by circularly polarized light," Phys. Rev. Lett. **86**, 1187–1190 (2001).

[6] C. Lux, M. Wollenhaupt, T. Bolze, Q. Liang, J. Koehler, C. Sarpe, and T. Baumert, "Circular dichroism in the photoelectron angular distributions of camphor and fenchone from multiphoton ionization with femtosecond laser pulses," Angew. Chem. Int. Ed. **51**, 5001–5005 (2012).

[7] M. H. M. Janssen and I. Powis, "Detecting chirality in molecules by imaging photoelectron circular dichroism," Phys. Chem. Chem. Phys. **16**, 856–871 (2014).

[8] A. Kastner, C. Lux, T. Ring, S. Züllighoven, C. Sarpe, A. Senftleben, and T. Baumert, "Enantiomeric excess sensitivity to below one percent by using femtosecond photoelectron circular dichroism," Chem. Phys. Chem. **17**, 1119–1122 (2016).

[9] A. Comby, E. Bloch, C. M. M. Bond, D. Descamps, J. Miles, S. Petit, S. Rozen, J. B. Greenwood, V. Blanchet, and Y. Mairesse, "Real-time determination of enantiomeric and isomeric content using photoelectron elliptical dichroism," Nat. Commun. **9**, 5212 (2018).

[10] R. Cireasa, A. E. Boguslavskiy, B. Pons, M. C. H. Wong, D. Descamps, S. Petit, H. Ruf, N. Thiré, A. Ferré, J. Suarez, J. Higuet, B. E. Schmidt, A. F. Alharbi, F. Légaré, V. Blanchet, B. Fabre, S. Patchkovskii, O. Smirnova, Y. Mairesse, and V. R. Bhardwaj, "Probing molecular chirality on a sub-femtosecond timescale," Nat. Phys. **11**, 654–658 (2015).

[11] O. Neufeld, D. Ayuso, P. Decleva, M. Y. Ivanov, O. Smirnova, and O. Cohen, "Ultrasensitive chiral spectroscopy by dynamical symmetry breaking in high harmonic generation," Phys. Rev. X **9**, 031002 (2019).

[12] D. Baykusheva and H. J. Wörner, "Chiral discrimination through bielliptical high-harmonic spectroscopy," Phys. Rev. X **8**, 031060 (2018).

[13] S. Beaulieu, A. Comby, A. Clergerie, J. Caillat, D. Descamps, N. Dudovich, B. Fabre, R. Géneaux, F. Légaré, S. Petit, B. Pons, G. Porat, T. Ruchon, R. Taïeb, V. Blanchet, and Y. Mairesse, "Attosecond-resolved photoionization of chiral molecules," Science **358**, 1288–1294 (2017).

[14] A. F. Ordonez and O. Smirnova, "Generalized perspective on chiral measurements without magnetic interactions," Phys. Rev. A **98**, 063428 (2018), arXiv:1806.09050 [physics].

[15] J. Gagnon, K. F. Lee, D. M. Rayner, P. B. Corkum, and V. R. Bhardwaj, "Coincidence imaging of polyatomic molecules via laser-induced Coulomb explosion," J. Phys. B **41**, 215104 (2008).

[16] C. S. Slater, S. Blake, M. Brouard, A. Lauer, C. Vallance, J. J. John, R. Turchetta, A. Nomerotski, L. Christensen, J. H. Nielsen, M. P. Johansson, and H. Stapelfeldt, "Covariance imaging experiments using a pixel-imaging mass-spectrometry camera," Phys. Rev. A **89**, 011401 (2014).

[17] M. Burt, K. Amini, J. W. L. Lee, L. Christiansen, R. R. Johansen, Y. Kobayashi, J. D. Pickering, C. Vallance, M. Brouard, and H. Stapelfeldt, "Communication: Gas-phase structural isomer identification by Coulomb explosion of aligned molecules," J. Chem. Phys. **148**, 091102 (2018).

[18] L. Christensen, J. H. Nielsen, C. S. Slater, A. Lauer, M. Brouard, and H. Stapelfeldt, "Using laser-induced Coulomb explosion of aligned chiral molecules to determine their absolute configuration," Phys. Rev. A **92**, 033411 (2015).

[19] A. Yachmenev and S. N. Yurchenko, "Detecting chirality in molecules by linearly polarized laser fields," Phys. Rev. Lett. **117**, 033001 (2016).

[20] I. Tutunnikov, E. Gershnabel, S. Gold, and I. Sh. Averbukh, "Selective orientation of chiral molecules by laser fields with twisted polarization," J. Phys. Chem. Lett. **9**, 1105–1111 (2018).

[21] A. Yachmenev, J. Onvlee, E. Zak, A. Owens, and J. Küpper, "Field-induced diastereomers for chiral separation," Phys. Rev. Lett. **123**, 243202 (2019), arXiv:1905.07166 [physics].

[22] A. A. Milner, J. A. M. Fordyce, I. MacPhail-Bartley, W. Wasserman, V. Milner, I. Tutunnikov, and I. S. Averbukh, "Controlled enantioselective orientation of chiral molecules with an optical centrifuge," Phys. Rev. Lett. **122**, 223201 (2019).

[23] Z. Vager, R. Naaman, and E. P. Kanter, "Coulomb explosion imaging of small molecules," Science **244**, 426–431 (1989).

[24] R. B. de Castilho, T. C. Ramalho, C. V. Nunez, L. H. Coutinho, A. C. F. Santos, S. Pilling, A. F. Lago, M. O. Silva-Moraes, and G. G. B. de Souza, "Single and double ionization of the camphor molecule excited around the C 1s edge," Rapid Commun. Mass Spectrom. **28**, 1769–1776 (2014).

[25] A. Owens and A. Yachmenev, "RichMol: A general variational approach for rovibrational molecular dynamics in external electric fields," J. Chem. Phys. **148**, 124102 (2018), arXiv:1802.07603 [physics].

[26] Z. Kisiel, O. Desyatnyk, E. Białkowska-Jaworska, and L. Pszczółkowski, "The structure and electric dipole moment of camphor determined by rotational spectroscopy," Phys. Chem. Chem. Phys. **5**, 820–826 (2003).

[27] R. B. Sidje, "Expokit: a software package for computing matrix exponentials," ACM Trans. Math. Soft. **24**, 130–156 (1998).

[28] T. H. Dunning, "Gaussian basis sets for use in correlated molecular calculations. I. The atoms boron through neon and hydrogen," J. Chem. Phys. **90**, 1007 (1989).

[29] R. A. Kendall, T. H. Dunning, Jr., and R. J. Harrison, "Electron affinities of the first-row atoms revisited. Systematic basis sets and wave functions," J. Chem. Phys. **96**, 6796–6806 (1992).

[30] CFOUR, Coupled-Cluster techniques for Computational Chemistry, a quantum chemical program package written by J. F. Stanton, J. Gauss, M. E. Harding, and P. G. Szalay with contributions from A. A. Auer, R. J. Bartlett, U. Benedikt, C. Berger, D. E. Bernholdt, Y. J. Bomble, L. Cheng, O. Christiansen, M. Heckert, O. Heun, C. Huber, T.-C. Jagau, D. Jonsson, J. Jusélius, K. Klein, W. J. Lauderdale, D. A. Matthews, T. Metzroth, L. A. Mück, D. P. O'Neill, D. R. Price, E. Prochnow, C. Puzzarini, K. Ruud, F. Schiffmann, W. Schwalbach, S. Stopkowicz, A. Tajti, J. Vázquez, F. Wang, J. D. Watts, and the integral packages MOLECULE (J. Almlöf and P. R. Taylor), PROPS (P. R. Taylor), ABACUS (T. Helgaker, H. J. Aa. Jensen, P. Jørgensen, and J. Olsen), and ECP routines by A. V. Mitin and C. van Wüllen. For the current version, see `http://www.cfour.de` (2018).

[31] J. Wang, V. A. Shamamian, B. R. Thomas, J. M. Wilkinson, J. Riley, C. F. Giese, and W. R. Gentry, "Speed ratios greater than 1000 and temperatures less than 1 mK in a pulsed He beam," Phys. Rev. Lett. **60**, 696 (1988).

[32] M. Hillenkamp, S. Keinan, and U. Even, "Condensation limited cooling in supersonic expansions," J. Chem. Phys. **118**, 8699–8705 (2003).

[33] M. Johny, J. Onvlee, T. Kierspel, H. Bieker, S. Trippel, and J. Küpper, "Spatial separation of pyrrole and pyrrole-water clus-

ters," Chem. Phys. Lett. **721**, 149–152 (2019), arXiv:1901.05267 [physics].
[34]F. Filsinger, J. Küpper, G. Meijer, L. Holmegaard, J. H. Nielsen, I. Nevo, J. L. Hansen, and H. Stapelfeldt, "Quantum-state selection, alignment, and orientation of large molecules using static electric and laser fields," J. Chem. Phys. **131**, 064309 (2009), arXiv:0903.5413 [physics].
[35]Y.-P. Chang, D. A. Horke, S. Trippel, and J. Küpper, "Spatially-controlled complex molecules and their applications," Int. Rev. Phys. Chem. **34**, 557–590 (2015), arXiv:1505.05632 [physics].
[36]S. Trippel, M. Johny, T. Kierspel, J. Onvlee, H. Bieker, H. Ye, T. Mullins, L. Gumprecht, K. Długołęcki, and J. Küpper, "Knife edge skimming for improved separation of molecular species by the deflector," Rev. Sci. Instrum. **89**, 096110 (2018), arXiv:1802.04053 [physics].
[37]F. Filsinger, U. Erlekam, G. von Helden, J. Küpper, and G. Meijer, "Selector for structural isomers of neutral molecules," Phys. Rev. Lett. **100**, 133003 (2008), arXiv:0802.2795 [physics].
[38]O. Ghafur, A. Rouzée, A. Gijsbertsen, W. K. Siu, S. Stolte, and M. J. J. Vrakking, "Impulsive orientation and alignment of quantum-state-selected NO molecules," Nat. Phys. **5**, 289–293 (2009).
[39]S. Y. T. van de Meerakker, H. L. Bethlem, N. Vanhaecke, and G. Meijer, "Manipulation and control of molecular beams," Chem. Rev. **112**, 4828–4878 (2012).
[40]M. Hartmann, R. E. Miller, J. P. Toennies, and A. F. Vilesov, "High-resolution molecular spectroscopy of van der waals clusters in liquid helium droplets," Science **272**, 1631–1634 (1996).
[41]A. Chatterley, B. Sheperson, and H. Stapelfeldt, "Three-dimensional molecular alignment inside helium nanodroplets," Phys. Rev. Lett. **119**, 073202 (2017).
[42]A. S. Chatterley, C. Schouder, L. Christiansen, B. Shepperson, M. H. Rasmussen, and H. Stapelfeldt, "Long-lasting field-free alignment of large molecules inside helium nanodroplets," Nat. Commun. **10**, 073202 (2019).
[43]N. R. Hutzler, H.-I. Lu, and J. M. Doyle, "The buffer gas beam: An intense, cold, and slow source for atoms and molecules," Chem. Rev. **112**, 4803–4827 (2012), arXiv:1111.2841 [physics].
[44]J. D. Weinstein, R. deCarvalho, T. Guillet, B. Friedrich, and J. M. Doyle, "Magnetic trapping of calcium monohydride molecules at millikelvin temperatures," Nature **395**, 148–150 (1998).
[45]D. Patterson and J. M. Doyle, "A slow, continuous beam of cold benzonitrile," Phys. Chem. Chem. Phys. **17**, 5372–5375 (2015).
[46]A. K. Samanta, M. Amin, A. D. Estillore, N. Roth, L. Worbs, D. A. Horke, and J. Küpper, "Controlled beams of shockfrozen, isolated, biological and artificial nanoparticles," Struct. Dyn. **7**, 024304 (2020), arXiv:1910.12606 [physics].
[47]L. Christensen, L. Christiansen, B. Shepperson, and H. Stapelfeldt, "Deconvoluting nonaxial recoil in Coulomb explosion measurements of molecular axis alignment," Phys. Rev. A **94**, 023410 (2016).
[48]T. Mullins, E. T. Karamatskos, J. Wiese, J. Onvlee, A. Yachmenev, A. Rouzée, S. Trippel, and J. Küpper, "Toward three-dimensional field-free alignment of arbitrary asymmetric top molecules," (2020), in preparation.
[49]B. Friedrich and D. Herschbach, "Enhanced orientation of polar molecules by combined electrostatic and nonresonant induced dipole forces," J. Chem. Phys. **111**, 6157 (1999).
[50]L. Holmegaard, J. H. Nielsen, I. Nevo, H. Stapelfeldt, F. Filsinger, J. Küpper, and G. Meijer, "Laser-induced alignment and orientation of quantum-state-selected large molecules," Phys. Rev. Lett. **102**, 023001 (2009), arXiv:0810.2307 [physics].
[51]I. Nevo, L. Holmegaard, J. H. Nielsen, J. L. Hansen, H. Stapelfeldt, F. Filsinger, G. Meijer, and J. Küpper, "Laser-induced 3D alignment and orientation of quantum state-selected molecules," Phys. Chem. Chem. Phys. **11**, 9912–9918 (2009), arXiv:0906.2971 [physics].
[52]L. V. Thesing, J. Küpper, and R. González-Férez, "Time-dependent analysis of the mixed-field orientation of molecules without rotational symmetry," J. Chem. Phys. **146**, 244304 (2017), arXiv:1705.03225 [physics].
[53]H. Stapelfeldt and T. Seideman, "Colloquium: Aligning molecules with strong laser pulses," Rev. Mod. Phys. **75**, 543–557 (2003).
[54]S. Trippel, T. Mullins, N. L. M. Müller, J. S. Kienitz, K. Długołęcki, and J. Küpper, "Strongly aligned and oriented molecular samples at a kHz repetition rate," Mol. Phys. **111**, 1738 (2013), arXiv:1301.1826 [physics].
[55]L. Nahon, L. Nag, G. A. Garcia, I. Myrgorodska, U. Meierhenrich, S. Beaulieu, V. Wanie, V. Blanchet, R. Géneaux, and I. Powis, "Determination of accurate electron chiral asymmetries in fenchone and camphor in the VUV range: sensitivity to isomerism and enantiomeric purity," Phys. Chem. Chem. Phys. **18**, 12696–12706 (2016).
[56]J. Ullrich, R. Moshammer, A. Dorn, R. Dörner, L. P. H. Schmidt, and H. Schmidt-Böcking, "Recoil-ion and electron momentum spectroscopy: Reaction-microscopes," Rep. Prog. Phys. **66**, 1463–1545 (2003).